Fuel 377 (2024) 132583

Contents lists available at ScienceDirect

Fuel

journal homepage: www.elsevier.com/locate/fuel

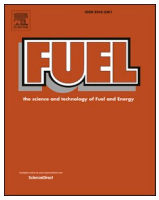

Full Length Article

Dew points for hydrogen-rich (hydrogen + propane) and (hydrogen + *n*-butane) mixtures determined with a microwave re-entrant cavity resonator

Yvonne Leusmann [a], Sebastian Klink [a], David Vega-Maza [b], Markus Richter [a,*]

[a] *Applied Thermodynamics, Chemnitz University of Technology, 09107 Chemnitz, Germany*
[b] *Energy Engineering and Fluid Mechanics, BioEcoUVa, University of Valladolid, 47011 Valladolid, Spain*

ARTICLE INFO

Keywords:
Butane
Dew-point measurements
Hydrocarbons
Hydrogen
Microwave re-entrant cavity resonator
Mixture
Propane

ABSTRACT

Dew-point measurements were performed for hydrogen-rich binary mixtures with hydrocarbon mole fractions of 0.09995 C_3H_8, 0.1499 C_3H_8, 0.0513 n-C_4H_{10}, and 0.09888 n-C_4H_{10} using a modified microwave re-entrant cavity apparatus. Isochoric measurements were conducted in the temperature range of (256 to 286) K with pressures up to 6.8 MPa and 2.0 MPa for mixtures containing propane and *n*-butane, respectively. The combined expanded uncertainties ($k = 2$) in dew-point temperature and pressure were estimated to be between (0.35 and 2.0) K and (0.0011 and 0.030) MPa. The agreement with predictions of the GERG-2008 equation of state is within 5.5%. However, better agreement with predicted values was achieved using a cubic equation recently developed in-house. Moreover, experiments with short- and long-term exposure of pressure sensors to hydrogen have shown that pressure measurement, and thus the uncertainty, can be affected; further investigation on this matter is therefore inevitable to improve hydrogen thermophysical property data.

1. Introduction

Climate change mitigation requires replacing fossil natural gas with energy gases derived from renewable sources when other low-carbon technologies are not available. Any blend of renewable gases presents new challenges for harmonizing gas quality within existing networks. Therefore, a better understanding of the thermodynamic properties of these gas mixtures is needed for supporting metrological capability, regulatory legislation, and engineered solutions, which in turn enables wider adoption.

The injection of hydrogen into the gas grid at various concentrations from renewable sources (Power-to-Gas) provides a solution for decarbonizing the grid and a pathway for the chemical storage of intermittent renewable energy sources. As a fuel additive for gasoline engines, hydrogen can improve the efficiency and performance of those and therewith reduce exhaust emissions and fuel consumption [1]. Within this new energy paradigm, gas grids and geological storages can balance energy supply and demand. The injection, transportation, and storage of Hydrogen-Enriched Natural Gas blends (HENG) necessitate accurate thermodynamic and transport properties across a wide range of temperatures, pressures, and compositions. These properties are typically derived from calibrated and validated models complemented by consistent measurements with known experimental uncertainties. However, a significant hydrogen content in natural gas mixtures can lead to substantial discrepancies between experimental data and model predictions [2–4]. This is because thermodynamic models have primarily been optimized for calculating the thermophysical properties of 'conventional' natural gas mixtures. Addressing this gap is crucial, and models need to be adapted to accommodate the diversity of these mixtures. This requires both, high-quality thermophysical property data and its corresponding implementation within the models.

The current reference equation of state (EOS) for natural gases is the GERG-2008 EOS by Kunz and Wagner [5], as mentioned in the international standard ISO 20765–2. It already considers "natural gases containing high fractions of hydrogen" by integration of a binary-specific departure function for the methane-hydrogen system, however, for all other hydrogen-hydrocarbon systems, only adjusted reducing functions or linear combining rules are used. Nevertheless, the first steps towards improvement have already been taken. For instance, the GERG-2008 EOS was developed further for methane-rich mixtures in the cryogenic regime [6], and predictions for the binary mixtures of hydrogen in combination with CO_2, N_2, CH_4, and CO were improved [7]. H_2 + {Ar, He, Ne} have

* Corresponding author.
E-mail address: m.richter@mb.tu-chemnitz.de (M. Richter).

https://doi.org/10.1016/j.fuel.2024.132583
Received 22 May 2024; Received in revised form 14 July 2024; Accepted 19 July 2024
Available online 16 August 2024

also been optimized recently [8]. However, binary hydrogen mixtures of C_3H_8 and n-C_4H_{10} have not yet been considered.

Among the alkanes, only the $H_2 + CH_4$ binary mixture entails a binary-specific departure function within the GERG-2008 EOS [5], an expanded version of the previous GERG-2004 EOS [9], both multiparameter fundamental Helmholtz energy EOS. For the ($H_2 + C_3H_8$) and ($H_2 + n$-C_4H_{10}) systems, only reducing functions were fitted. Low-uncertainty experimental data for these systems are needed to enable the development of binary-specific departure functions and hence improve the accuracy of the predictions of the GERG model.

Beyond data for the homogeneous phases, vapor–liquid equilibrium (VLE) data for the ($H_2 + C_3H_8$) and ($H_2 + n$-C_4H_{10}) systems are key to further developing mixture EOS. Vapor saturation conditions, i.e., dew points, are critical to avoid multiphase flow under transport conditions, a requirement for ensuring optimized gas flow through the gas infrastructure. Determining the dew line at different H_2 concentrations is therefore crucial, as even small H_2 concentrations can significantly alter the phase behavior of these blends [10]. However, a comprehensive understanding of this critical phenomenon is hindered by the scarcity and inconsistency of existing experimental data and discrepancies within the industry's most widely used models.

Robust, accurate, and repeatable measurements of dew points with small sample volumes are needed to allow for safe operation with explosive gas mixtures such as hydrogen-rich fluids. Measurements based on microwave resonant techniques offer a reliable and sensitive method for detecting small quantities of liquid in a gas phase, i.e., dew points. Typically, it is more sensitive and with higher resolution at detecting a phase change, e.g., compared to traditional isochoric techniques. It can also perform online measurements. These measurements depend on the volume and not just the surface [11]. Moreover, working with gravimetrically prepared gas mixtures, as a synthetic approach, provides low uncertainty in composition, which is a significant source of error in analytical techniques. Our previous experience [12–15] established that the microwave-based measuring principle using a re-entrant cavity offers low uncertainty and, in principle, a fast technology for measuring VLE. Here, the dew point is determined by a slope discontinuity of resonant frequency versus temperature when crossing the phase boundary. Previous authors laid the groundwork with their seminal work [16–20]. Furthermore, re-entrant cavities offer accurate measurements in a less demanding experimental approach compared to other microwave techniques, such as quasi-spherical microwave resonators [21,22]. A custom design of re-entrant cavities, modeled as a parallel *RLC* circuit, can leverage the inherent qualities of this detection technique to materialize an effective and robust dew-point detector across a wide range of temperatures, pressures, and compositions. Moreover, this technique allows for the investigation of phase densities, dielectric permittivities, and liquid volume fractions [17–19], as recently further developed by Leusmann *et al.* [23].

In the present work, we present dew-point measurements of four hydrogen-rich binary mixtures containing either propane or *n*-butane, measured with a microwave re-entrant cavity system. The results are compared with the GERG-2008 EOS [5] and a new cubic EOS developed by Yang *et al.* [24], as well as with experimental data retrieved from the literature.

2. Experimental

2.1. Apparatus Description

The experimental system used in this work is based on the microwave re-entrant cavity resonator built by the National Engineering Laboratory (NEL, East Kilbride, UK) [25], with a design adapted to the 'classic' cavity design developed by Goodwin *et al.* [17]. While the original apparatus was not specifically designed and built to measure phase equilibrium data (see Tsankova *et al.* [12]), it has proven to deliver reliable and accurate results in the past decade after being refurbished at Ruhr University Bochum (RUB) [13–15]. To continue improving the quality of measurements, further modifications were made at Chemnitz University of Technology (TUC), the present location of the microwave apparatus. Table 1 summarizes the main modifications. The experimental setup and methods used have been described in great detail by Tsankova *et al.* [12], and only aspects regarding recent modifications are elucidated below. The upgraded apparatus enables measurements over a temperature and pressure range of (253 to 353) K and up to 12 MPa, respectively.

Re-entrant cavity resonator

The design of the re-entrant cavity resonator has not been updated and remains as is (see Section 2.1 of Tsankova *et al.* [12]).

Resonant frequency measurement

The vector network analyzer (VNA) used to measure the complex transmission coefficient S_{21} to determine the resonance frequencies of the system was updated (Keysight, Model: E5063A) and now has a larger frequency range of (0.1 to 8.5) GHz compared to the previous maximum frequency of only 1.3 GHz. This is particularly useful for investigating the resonator's higher-order modes of relevance in new cavity designs. The basic settings of the VNA necessary for frequency measurements when studying dew points can be found in the SI (Table S1).

Temperature measurement and control

The temperature measurement chain of the system has been replaced with a 100 Ω platinum resistance thermometer (PRT, Fluke, Model: 5606), protruding down into the bulb of the cavity, and a precision thermometry bridge (Anton Paar, Model: MKT 50), recording the resistance of the thermometer. The expanded measurement uncertainty ($k = 2$) of the PRT stated in the manufacturer's calibration certificate is 0.01 K and was validated on site at the triple point of water, according to ITS-90. The expanded uncertainty ($k = 2$) of the thermometry bridge, as stated by the manufacturer, is 1 mK. The combined expanded uncertainty ($k = 1.73$) in temperature was estimated to be less than 25 mK. The contributions included in this estimation are described in Section 3.2.

For controlling and monitoring the measuring cell temperature, the same modified bath thermostat and temperature controller are used as previously employed (Grant, Model: LTX-2006–40 and Eurotherm, Model: 2416). The stability of the bath thermostat after equilibration is 5–10 mK, depending on the target temperature. For details of the previously used temperature measuring chain, including temperature control, we refer to Section 2.4 of the work of Tsankova *et al.* [12].

Pressure measurement

The pressure measurement has not been updated and remains as is (for details see Section 2.5 of Tsankova *et al.* [12]): A pressure cascade consisting of three quartz oscillator pressure transducers (Paroscientific, Models: 223A-101, 2100A-101, and 42 K-CE) was used that covered the instrument's operational pressure range in three subranges that overlapped with maximum pressures (0.69, 2.7 and 13.8) MPa. The

Table 1
Modifications and updates of the current microwave setup at TUC (2023) compared to the RUB apparatus setup (2016). For easy comparison, the listed items are identical or similar in name to those described by Tsankova *et al.* [12].

Item	Modifications/Updates made at TUC as of 2023
Re-entrant Cavity Resonator	None
Resonant Frequency Measurement	New vector network analyzer, new microwave cables
Temperature measurement and control	Different temperature sensors, different resistance bridge
Pressure measurement	None
DAQ Software	New DAQ code (LabView)
Add-on's	Syringe pump

Table 2
Molar composition, expanded uncertainties ($k = 2$), and pure component purity provided by the supplier for the ($H_2 + C_3H_8$) and ($H_2 + n$-C_4H_{10}) mixture investigated in this work.

Chemical name	CAS no.	Supplier	Purity / Mole fraction $x_{C3H8/n\text{-}C4H10}$	Purification method
n-Butane	106–97–8	Air Liquide	n/a[a]	None
Hydrogen	1333–74–0	Air Liquide	n/a[a]	None
Propane	274–98–6	Air Liquide	n/a[a]	None
Mixtures $H_2 + C_3H_8$:				
Mixture 1	n/a	Air Liquide	0.09995 ± 0.00050[a]	unknown[a]
Mixture 2	n/a	Air Liquide	0.14990 ± 0.00150[a]	unknown[a]
Mixtures $H_2 + n$-C_4H_{10}:				
Mixture 3	n/a	Air Liquide	0.05130 ± 0.00051[a]	unknown[a]
Mixture 4	n/a	Air Liquide	0.09888 ± 0.00100 [a]	unknown[a]

[a] Impurities and analysis method for composition not stated by the supplier.

combined expanded uncertainty ($k = 1.73$) as stated by the manufacturer is 0.01% full scale. All pressure transducers were thermostated at $T = 318.15$ K to minimize the impacts associated with changes in laboratory temperature, as well as the condensation and sorption effects of the sample fluid.

DAQ software

A new code has been implemented with the software LabVIEW of National Instruments [26] to monitor, record, and store raw data. Compared to the previous DAQ method, a higher degree of automation has been employed, which is less prone to error with regard to data handling. Furthermore, we have applied a post-processing fitting algorithm to the frequency measurement that uses the *Q*-circle method to determine the actual local maximum of a resonance mode – this is needed for the determination of dew points (see Section 3).

Add-on's

For the ($H_2 + C_3H_8$) and ($H_2 + n$-C_4H_{10}) mixtures investigated in this work, a syringe pump (Teledyne ISCO, Model: 260D) has been integrated into the experimental setup. Using the syringe pump, measurements above the initial cylinder pressure provided by the manufacturer were enabled while paying close attention to strictly staying in the single-phase region.

2.2. Materials

All four mixtures were prepared by Air Liquide at SAPHIR quality with the pure components, mixture compositions, and uncertainties specified in Table 2. Each mixture was delivered with a certificate specifying the expanded uncertainty in composition at a coverage factor of $k = 2$ for all mixtures. No details on the analysis method of the final compositions could be provided by the supplier. However, we assume that gas chromatography was utilized since it is the common analytical method for such gas mixtures. The propane mole fractions for the ($H_2 + C_3H_8$) mixtures were stated as (0.09995 ± 0.00050) and (0.14990 ± 0.00150), and the *n*-butane mole fractions for the ($H_2 + n$-C_4H_{10}) mixtures were stated as (0.05130 ± 0.00051) and (0.09888 ± 0.00100). Although the filling pressures of the gas cylinders were agreed upon with the supplier within the joint project, the filling strategy was kept conservative so that the cylinders were filled to maximum pressures very far below the supposed dew line. As a result, the filling pressures turned out to be quite low in some cases.

2.3. Measuring procedure and sample handling

As a first step, for each individual mixture, the apparatus was evacuated at $T = T_a \approx 295$ K using a rotary vane pump (Leybold vacuum, TRIVAC D 1.2 D) and then flushed 3 times to eliminate residuals and

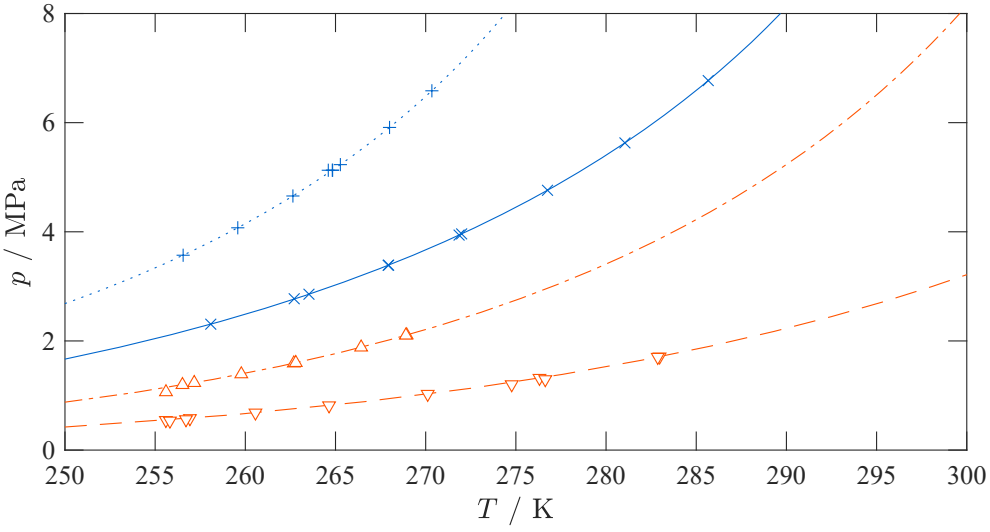

Fig. 1. *p*, *T*-diagram of two ($H_2 + C_3H_8$) and two ($H_2 + n$-C_4H_{10}) mixtures showing the dew points measured in this work. The phase boundaries were calculated with the GERG-2008 EOS of Kunz and Wagner [5]. Lines indicate calculated phase boundaries, and symbols represent respective experimental dew points: · · ·, +, Mixture 1 (0.9 H_2 + 0.10 C_3H_8); ——, ×, Mixture 2 (0.85 H_2 + 0.15 C_3H_8); – · –, △, Mixture 3 (0.95 H_2 + 0.05 n-C_4H_{10}); – –, ▽, Mixture 4 (0.90 H_2 + 0.10 n-C_4H_{10}).

avoid changes in the composition caused by sorption effects [27]. Dew points were measured along an isochoric pathway, and for each dew point, the measuring cell was filled with fresh sample at $T \approx 303$ K and a filling rate of ~ 0.06 MPa·min^{-1}. Where necessary, a syringe pump was used to achieve pressures higher than the maximum cylinder filling pressure provided by the manufacturer to increase the overall measuring range (T, p), carefully avoiding the two-phase region during the filling process. The sample cylinder was heated before each filling to homogenize the sample.

Dew points along an isochoric pathway were measured with respect to temperature decrements of 0.2 K, spanning an interval of approximately 5 K (~25 steps). Starting and stopping 2.5 K above and below the assumed dew point ($T_{dew} + 2.5$ K $> T_{dew} > T_{dew} - 2.5$ K), the temperature was gradually decreased while the system was allowed to equilibrate at each step. Equilibrium was achieved when the temperature, pressure, and frequency became constant within predefined limits of 0.01 K, 0.001 MPa and 0.01 MHz over 20 min. At each equilibrium point (T, p, f), data were recorded approximately every second for 5–10 min and then averaged. After measuring all (~25) steps of an isochor, the temperature was increased for the fluid mixture to return to the single-phase region and then fully vented before refilling the system. A fresh refill was necessary to avoid a change in the composition of the investigated sample after the phase boundary was crossed and the mixture was returned to the single-phase vapor region. The mathematical determination of the dew point via the collected data is described in Section 3.

The dew points measured in this work range from $T = (256$ to $286)$ K, $p \leq 6.8$ MPa for the ($H_2 + C_3H_8$) mixtures and $T = (256$ to $283)$ K, $p \leq 2.0$ MPa for the ($H_2 + n$-C_4H_{10}) mixtures. Fig. 1 shows the phase envelope of the four investigated mixtures calculated with the GERG-2008 EOS of Kunz and Wagner [5] as implemented in REFPROP [28] and the location at which the dew points were determined.

While it is strongly advised to calibrate the microwave resonator prior to certain measurements, we would like to note that a resonator calibration is not necessary when conducting dew-point measurements only. Therefore, no resonator calibration was performed in this work. Taking the measurement of the dielectric permittivity, ε, as an example, the effects of thermal expansion and pressure distortion of the resonator on the vacuum frequency are of great importance and must therefore be characterized accurately via calibration. Here, the equation to calculate ε includes several vacuum-depending values; hence, vacuum measurements (and underlying calibration of those) have a direct impact on ε (see Tsankova *et al.* [13] for details). This is not true for dew-point determination, where only a shift in the resonance frequency is measured (see Section 3).

3. Dew-Point Determination

3.1. Dew-point determination from frequency measurements

The key measured variable of an apparatus with microwave cavities is the resonant frequency, f, or several frequencies, f_i. It has an inverse dependence on the square root of the dielectric permittivity, ε, of a fluid and, subsequently, the density and composition. When approaching the dew point in the described way (isochoric cooling of the sample across the phase boundary, see Section 2.3), the density in the gas phase is nearly constant, resulting in an almost constant dielectric permittivity and resonant frequency. This changes abruptly when crossing the dew line caused by the onset of liquid formation of the less volatile component at the bottom of the measuring cell. Consequently, the density and co-depending dielectric permittivity of the remaining vapor sample decrease, which in turn leads to an increase in resonant frequency. The slope discontinuity of resonant frequency, when the phase boundary is crossed, can be used to determine the dew point. Here, the intersection of straight lines regressed to the single-phase and two-phase data results in the dew point. More detailed information on measuring fluid-mixture dew points with a microwave cavity can be found in the previous work of Tsankova *et al.* [12].

The resonant frequency used to determine the dew point can be obtained either by (1) measuring the frequency directly using the VNA or by (2) measuring the complex transmission coefficient S_{21} and afterwards fitting it to a Q-circle algorithm that is based on the phase versus frequency approach described in Petersan and Anlage [29]. While Tsankova *et al.* [12–15] have previously used (1) direct frequency measurements for dew point determination, we have used method (2) in this work. Fitting the complex transmission coefficient results in a more accurate determination of the local maximum (= resonant frequency) because the fitting algorithm interpolates between data points (S_{21}) to find the optimal maximum, while the direct measurements via VNA only return the highest measured value of S_{21} as the maximum. S_{21} was measured at 401 frequencies spanning an interval of 5–10 MHz. Only the fundamental resonant mode of the cavity, here Mode 1 ($\approx$ 390 MHz), was measured. Below, we provide a compact guidance of the key aspects for dew-point determination in this work:

1. Measure and record S_{21} vs. f (Mode 1), T, p data in 0.2 K steps for ($T_{dew} + 2.5$ K $> T_{dew} > T_{dew} - 2.5$ K)
2. Fit S_{21} vs. f data with Q-circle algorithm to obtain f
3. For each T-step, average f, p, T data from 5-10 min
4. Fit straight lines to single-phase and two-phase data to calculate intersection (= dew point)

3.2. Uncertainty analysis

The measurement uncertainty of dew-point temperature and pressure was determined following the method of the previous work by Tsankova *et al.* [12] with adaptions made where necessary. In accordance with the "Guide to the Expression of Uncertainty in Measurement" [30], the combined standard uncertainty in dew point temperature $u_c(T_{dew})$ and pressure $u_c(p_{dew})$ can be determined using equations (1) and (2), with all contributors described in Table 3. For the estimation of the combined expanded uncertainty $U_c = u_c \cdot k$, a coverage factor of $k = 2$ was assumed for both, temperature and pressure.

$$u_c(T_{dew}) = \left[u(T_{meas})^2 + u(T_{intersect})^2 + u(T_{repro})^2 + u(T(\mathrm{x}))^2 \right]^{1/2} \quad (1)$$

$$u_c(p_{dew}) = \left[u(p_{meas})^2 + \left(\left(\frac{\partial p}{\partial T} \right)_x \cdot u_c(T_{dew}) \right)^2 \right]^{1/2} \quad (2)$$

The standard uncertainty of the temperature measurement chain $u(T_{meas})$ is composed of various contributions: the individual standard uncertainty of the PRT (also involving the calibration) and its self-heating, the

Table 3
Uncertainty contributors for the determination of the combined standard uncertainty in dew-point temperature $u_c(T_{dew})$ and pressure $u_c(p_{dew})$, eqs. (1) and (2) , according to Tsankova's method [12]. x_{C_i} refers to the mole fraction of C_3H_8 or n-C_4H_{10}, depending on the mixture under investigation.

Uncertaintycontributor	Description
$u(T_{meas})$	standard uncertainty of the temperature measurement chain
$u(T_{intersect})$	uncertainty of the calculated intersection of two linear fits
$u(T_{repro})$	$= a \cdot T_{dew}$ = uncertainty based on the reproducibility of the measurements, where a is (0.4% for Mixture 1, 0.05% for Mixture 2, 0.15% for Mixture 3, 0.1% for Mixture 4)
$u(T(\mathrm{x}))$	$= \left(\frac{\Delta T}{\Delta x_{C_i}} \cdot u(x_{C_i}) \right) =$ uncertainty in dew-point temperature resulting from compositional uncertainty
$u(p_{meas})$	uncertainty in pressure measurement
$\left(\frac{\partial p}{\partial T} \right)_x$	sensitivity coefficient - variation of pressure with change in temperature

resistance bridge, heat dissipation of the measuring cable, temperature gradient along the wall of the measuring cell, and the temperature oscillation over time. Here, the basic assumption is that such input quantities cannot be measured directly and, therefore, have been described by a symmetric, rectangular probability distribution with a coverage factor of $k = 1.73$. For the temperature range of $T = (256$ to $286)$ K, in which dew-point measurements were carried out, the standard uncertainty in temperature was estimated to be $u(T_{meas}) = 25$ mK $\cdot$ 1.73^{-1}.

As described in Section 3.1, the dew-point temperature was determined by calculating the intersection of the linear regressions with the single- and two-phase data. The uncertainty of the intersection $u(T_{intersect})$ of two linear fits, used for dew-point determination in the present work (see Section 3.1), was calculated using a method described by Filliben and McKinney [31].

The reproducibility of the dew-point measurements $u(T_{repro})$ was estimated to be $(0.05$ to $0.4)\% \cdot T_{dew}$, depending on the mixture under investigation (see Table 3). This is higher than previously evaluated by Tsankova *et al.* [12], who assumed $u(T_{repro})_{Tsankova} = 0.001\% \cdot T_{dew}$. The increase in the contribution to reproducibility is related to the study of hydrogen and the potential influence and unknown impact of such a substance on the measuring equipment, e.g., the pressure transducers. Various test measurements with pure hydrogen prior to this work have shown that hydrogen can influence the pressure measurement. Over several weeks, we conducted pure hydrogen experiments in the pressure range from (0.55 to 8) MPa at measuring cell temperatures of $T = (263$, 273, 293, 303) K, systematically selecting and repeating measuring points. During all measurements, the pressure transducers were thermostated at $T = 318.15$ K to avoid the impacts associated with changes in laboratory temperature, as well as the condensation and sorption effects of the sample fluid. Although we were not able to identify distinct patterns or eliminate the hydrogen influence by applying a post-fitting algorithm to the data, it became very clear that hydrogen has some kind of impact on the pressure measurement that cannot be neglected and, therefore, has to be accounted for in the uncertainty determination. There is a tendency of the pressure transducers to fully recover from hydrogen measurements, which was verified with measurements of a well-characterized gas (argon), before, in-between and after the pure hydrogen experiments, but without an identifiable pattern (i.e., duration of exposure to hydrogen on the pressure sensors). With these findings, we encourage further investigation on this matter as a crucial and inevitable part of improving hydrogen data. Note that our observation is true for the Paroscientific pressure transducers used in this work; other types of transducers from different manufacturers may behave differently.

The uncertainty in dew-point temperature arising from the uncertainty in mixture composition, $u(T(x))$, was taken into account by applying a simplified approach reported by Richter *et al.* [32] to the four binary mixtures investigated in this work. According to the equation provided in Table 3, $u(x_{Ci})$ corresponds to the uncertainty in the mole fraction of C_3H_8 or n-C_4H_{10} stated and provided by Air Liquid. ΔT is the difference in dew-point temperature calculated with the a given composition and a dew-point temperature calculated with a composition changed by Δx_{C_i}. In this work, Δx_{C_i} was set equal to $u(x_{Ci})$.

The standard uncertainty in pressure measurement $u(p_{meas})$ arises from the absolute uncertainty of the pressure transducers and their measuring range (pressure cascade). As stated in Section 2.1, the estimated uncertainty in pressure according to the manufacturer is $u(p_{meas}) = 0.01\% \cdot p_{max} \cdot 1.73^{-1}$, where p_{max} corresponds to the maximum pressure of the respective pressure sensor. The uncertainty related to hydrostatic pressure correction can be neglected. The partial derivative (in uncertainty analysis typically called sensitivity coefficient) $(\partial p/\partial T)_x$ represents the variation of pressure with changes in temperature and is calculated from a sensitivity analysis with the experimental values. Alternatively, a calculation with an equation of state is possible.

4. Results and Discussion

The experimental dew points and their corresponding uncertainty determined for the (H_2 + C_3H_8) and (H_2 + n-C_4H_{10}) mixtures under investigation are reported in the supplementary information as machine-readable files in the Property Information Format (PIF) as proposed by Bernardini *et al.* [33]. Experimental VLE data sets available in the literature for (H_2 + C_3H_8) mixtures [34–37] and (H_2 + n-C_4H_{10}) mixtures [38–41] are presented in Table 4, along with the measured temperature and pressure ranges, compositions, and uncertainties. A similar literature overview was published by Lozano *et al.* in 2022 [42] for a large number of mixtures containing hydrogen but with fewer literature sources for the mixtures and values relevant to this work.

For the mixtures under study containing propane, Mixture 1 (0.90005 H_2 + 0.09995 C_3H_8) and Mixture 2 (0.8501 H_2 + 0.1499 C_3H_8), the combined expanded uncertainties ($k = 2$) in dew-point temperature and pressure are estimated to be between (0.35 and 2.0) K and (0.005 and 0.030) MPa, respectively. The results of the measured dew-point pressures for the two (H_2 + C_3H_8) mixtures are presented in Fig. 2 (top panel) as relative deviations of experimental data from values calculated with the GERG-2008 EOS by Kunz and Wagner [5] plotted versus temperature. The relative deviations in dew-point pressures for Mixture 1 range from (–0.270 to –2.98)%, while those for Mixture 2 deviate between (1.24 and 2.87)%.

All relative deviations are well within the uncertainty of 5% stated by the authors of the GERG-2008 EOS. Considering a not negligible impact on the uncertainty in pressure due to the likely impact of hydrogen on the pressure transducers, as discussed in Section 3.2, this is a sound result, particularly when looking at the very widely scattered data from the literature. Furthermore, as mentioned before, the GERG-2008 EOS does not include a binary-specific departure function for the (H_2 + C_3H_8) system but only an adjusted reducing function. For both reasons, it is justified that the uncertainty reported by the authors of the EOS is rather large. Besides the need for further development of the EOS, which in turn leads to a demand for a larger basis of experimental data, it emphasizes the need for a more detailed investigation of the impact of hydrogen on pressure sensors as a potentially significant source in the uncertainty of pressure measurement. In general, the magnitude of the deviations grows with increasing temperature but overall appears scattered. Especially reproduction measurements seem unsystematic, which we assign to the potential impact of hydrogen on the pressure transducers. In the top panel of Fig. 2, we also show relative deviations of dew-point pressures calculated with the OilMixProp 1.0 software package developed within our group by Yang and Richter [43] from values calculated with the GERG-2008 EOS [5]. OilMixProp uses a new cubic EOS developed by Yang *et al.* [24], where the binary interaction parameter was set to zero for (H_2 + C_3H_8) mixtures. Relative deviations range between (0.20 and –2.04)% for Mixture 1 and between (0.20 and

Table 4
Review of experimental VLE data sets for (H_2 + C_3H_8) and (H_2 + n-C_4H_{10}) mixtures used to compare the experimental data reported within the present work. Lozano *et al.* recently published a similar summary [42], however, with fewer literature sources for the relevant mixtures. Literature sources added in this work are labeled with *.

Authors	T / K	p_{max} / MPa	y_{H2}	Uncertainty T_i, p_i, y_{H2}
H_2 + C_3H_8:				
Burriss *et al.* (1953) [34]	278–361	53	0.128–0.840	–/0.0014 MPa/–
Trust and Kurata (1971) [35]	248–348	19	0.259–0.846	n/a
Williams and Katz (1954) [36]*	255–297	7	0.413–0.864	n/a
Bolshakov & Linshits (1954) [37]*	248–298	13	0.320–0.868	n/a
H_2 + n-C_4H_{10}:				n/a
Klink *et al.* (1975) [38]	328–394	17	0.213–0.932	n/a
Nelson and Bonnell (1943) [39]	297–389	11	0.624–0.833	n/a
Aroyan and Katz (1951) [40]	228, 244	6	0.979–0.992	n/a
Augood (1957) [41]*	214, 273	19	0.955–0.966	n/a

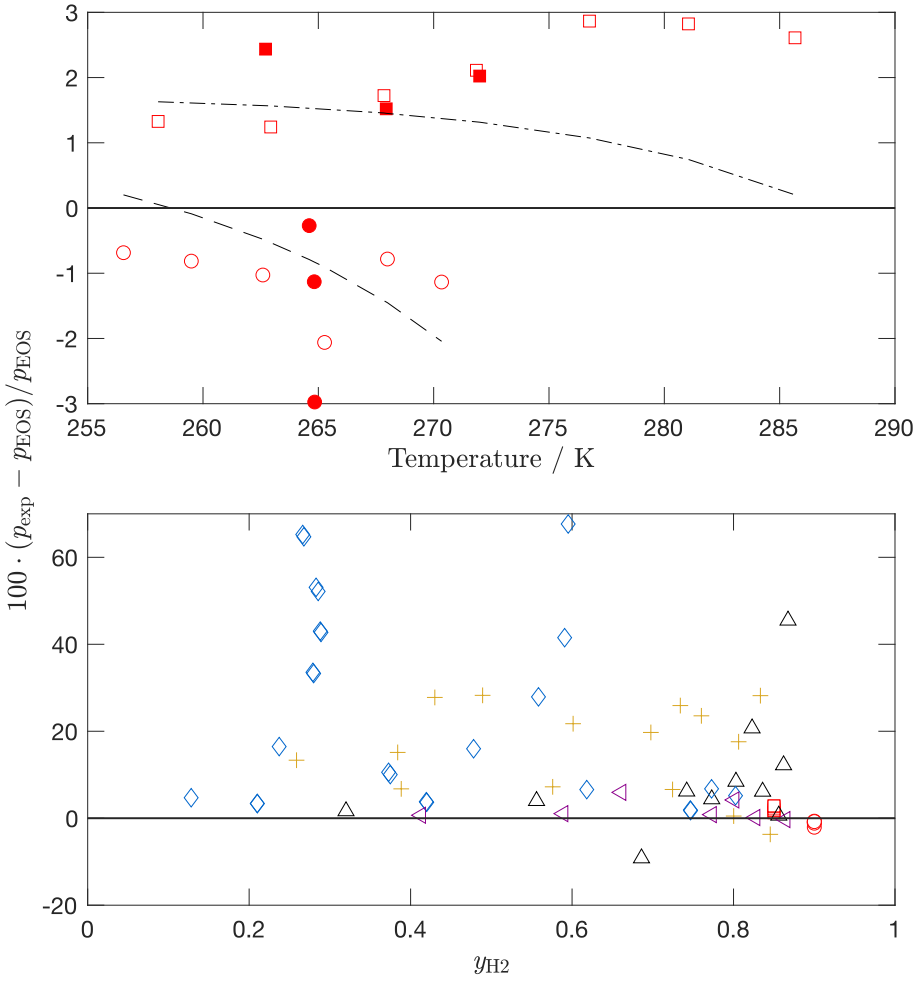

Fig. 2. Relative deviations of experimental dew-point pressures, p_{exp}, for (H_2 + C_3H_8) mixtures from dew-point pressures, p_{EOS}, calculated with the GERG-2008 EOS of Kunz and Wagner [5] (zero line) plotted versus temperature (top panel) and versus hydrogen vapor mole fraction y_{H2} (bottom panel). For both panels: ○, this work, Mixture 1 (0.90005 H2 + 0.09995 C_3H_8); □, this work, Mixture 2 (0.8501 H_2 + 0.1499 C_3H_8); ● and ■, reproduction measurements of the respective mixtures studied in this work; ◇, Burriss *et al.* [34]; +, Trust and Kurata [35]; ◁, Williams and Katz [36]; Δ, Bolshakov and Linshits [37]. Additionally, for the top panel: Relative deviations of dew-point pressures calculated with OilMixProp 1.0 [43] from values calculated with the GERG-2008 EOS plotted versus temperature for Mixture 1 (0.90005 H_2 + 0.09995 C_3H_8), – – –, and Mixture 2 (0.8501 H_2 + 0.1499 C_3H_8), – · –.

1.63)% for Mixture 2. The average relative deviation (ARD) of the experimental data of Mixture 1 from the GERG-2008 model is –1.21%, and for Mixture 2, the ARD is 2.07%. When comparing the experimental data with results predicted with OilMixProp, the ARD for Mixture 1 is only –0.41% and 0.83% for Mixture 2. Overall, the ARD is larger for predictions with the GERG-2008 EOS.

Fig. 2 (bottom panel) shows the relative deviations for (H_2 + C_3H_8) mixtures of experimental dew-point pressures and values calculated using the GERG-2008 EOS [5] plotted versus the hydrogen vapor mole fraction, for values measured in this work, as well as relevant VLE data retrieved from the literature [34–37] (see Table 4). In general, the relative deviations of experimental dew-point pressures found in the literature compared to the GERG-2008 EOS exhibit a wide range, with several points having relatively high deviations. For better visualization, relative deviations greater than 70% compared to the GERG-2008 EOS [5] are not shown in Fig. 2. No clear trends are identifiable, but rather scattering behavior dominates the data basis, with the exception of data reported by Burriss *et al.* [34]. Their experimental values show higher relative deviations with an increase in pressure ($p > 10$ MPa, rel. dev. > 50%). The dew-point pressures published by Williams and Katz [36] are in good agreement with our new experimental data, deviating from the zero line from (–0.1 to 6.0)% at y_{H2} between (0.413 and 0.910). Overall, the dew points determined in the current work are partly consistent with, but to a large extent better than those reported in the literature for (H_2 + C_3H_8) mixtures.

The new experimental data for the mixtures investigated in this work containing *n*-butane, Mixture 3 (0.9487 H_2 + 0.0513 *n*-C_4H_{10}), and Mixture 4 (0.9011 H_2 + 0.0989 *n*-C_4H_{10}) have yielded combined expanded uncertainties ($k = 2$) in dew-point temperature and pressure of (0.38 to 0.58) K and (0.001 to 0.004) MPa, respectively. Fig. 3 (top panel) shows the relative deviations of measured dew-point pressures for the two (H_2 + *n*-C_4H_{10}) mixtures from values calculated with the GERG-2008 EOS by Kunz and Wagner [5] plotted versus temperature. The relative deviations in dew-point pressures for Mixture 3 range from (–5.50 to 1.48)%, while those for Mixture 4 deviate between (1.34 and 12.92)%. For Mixture 3, the deviations are, for the most part, well within the uncertainty of 5% reported by Kunz and Wagner [5] with the exception of a single reproduction measurement, where the relative deviation is slightly higher (5.50%) and exceeds the otherwise consistent lower range of relative deviations of (−2.83 to 1.48)%. For Mixture 4, two trends are identifiable: (1) measurements conducted without using an ISCO pump to increase the pressure show a rather consistent picture of relative deviations between (1.34 and 3.68)%, while (2) measurements conducted employing an ISCO pump to achieve higher pressures result in larger relative deviations in dew-point pressures of (5.94 to 12.92)% (Fig. 3 top panel, highlighted with a dashed box). We

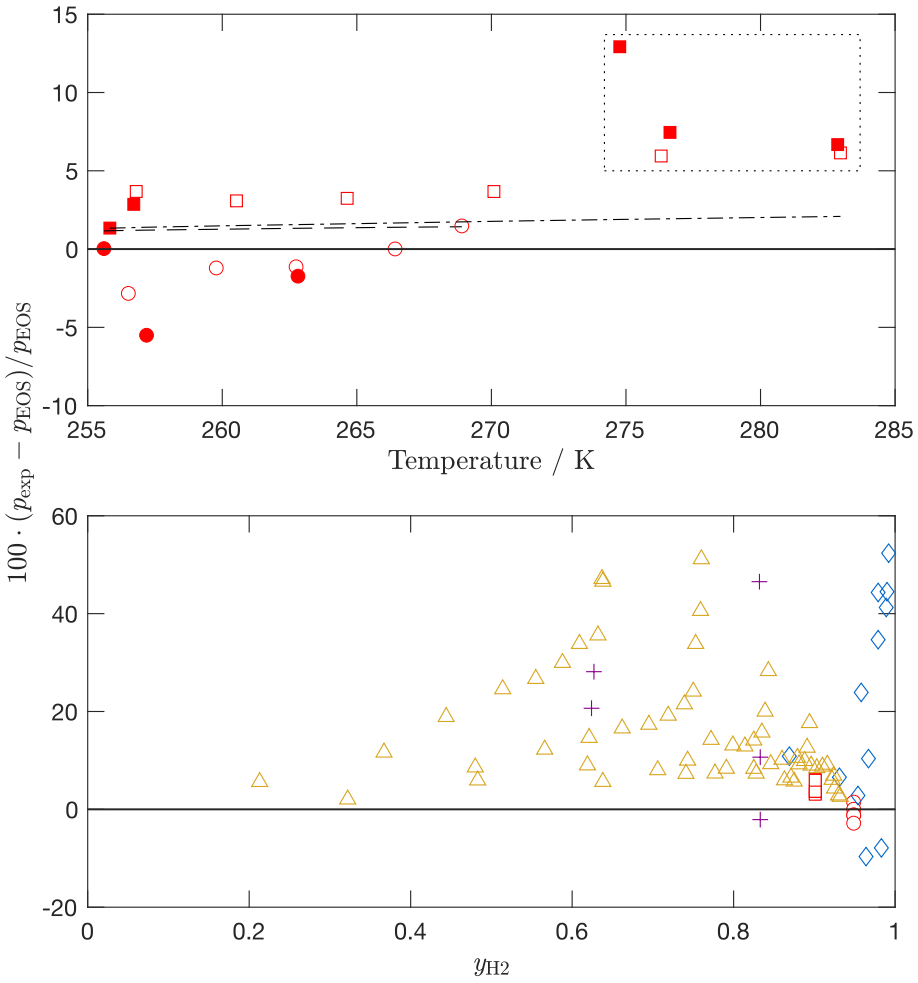

Fig. 3. Relative deviations of experimental dew point pressures, p_{exp}, for (H_2 + n-C_4H_{10}) mixtures from dew point pressures, p_{EOS}, calculated with the GERG-2008 EOS of Kunz and Wagner [5] (zero line) plotted versus temperature (top panel) and versus hydrogen vapor mole fraction y_{H2} (bottom panel). For both panels: ○, this work, Mixture 3 (0.9487 H_2 + 0.0513 n-C_4H_{10}); □, this work, Mixture 4 (0.9011 H_2 + 0.0989 n-C_4H_{10}); ● and ■, reproduction measurements of the respective mixtures measured in this work; ◇, Aroyan and Katz [40]; +, Nelson and Bonnell [39]; △, Klink *et al.* [38]. The dashed box (···) includes corrupted measuring data not further considered in this work. Additionally, for the top panel: Relative deviations of dew-point pressures calculated with OilMixProp 1.0 [43] from values calculated with the GERG-2008 EOS plotted versus temperature for Mixture 3 (0.9487 H_2 + 0.0513 n-C_4H_{10}), – – –, and Mixture 4 (0.9011 H_2 + 0.0989 n-C_4H_{10}), – · –.

relate the higher relative deviations of (2) to the utilization of the ISCO pump and, therewith, the potential of the mixture entering the two-phase region when compressing the gas to achieve higher pressure during the filling process of the apparatus. While all necessary parts were heated to T = 303 K, an issue with the implementation of such heating cannot be fully excluded.

For both mixtures, Mixture 3 and Mixture 4, it is also important to note that, as for the (H_2 + C_3H_8) system, the GERG-2008 EOS of Kunz and Wagner [5] does not include a binary-specific departure function for the (H_2 + n-C_4H_{10}) system, but an adjusted reducing function. Like the investigated mixtures containing propane (Mixtures 1 and 2), the impact on the uncertainty in dew-point pressures due to the likely impact of the pressure transducers being exposed to hydrogen (see Section 3.2) shall not be neglected and can play a significant role in the uncertainty estimation. As a result, two key factors for the improvement of uncertainties in dew-point pressure measurements are identified: the need for further development of the associated EOS, which in turn leads to the demand for a larger basis of experimental data and the need for a more detailed investigation on the impact of hydrogen on pressure sensors as a potentially significant source in the uncertainty of pressure measurement. The top panel of Fig. 3 also shows the relative deviations of dew-point pressures calculated with new cubic EOS developed by Yang *et al.* [24] (binary interaction parameter for (H_2 + n-C_4H_{10}) mixtures set to zero) as implemented in the software package OilMixProp 1.0 [43] from values calculated with the GERG-2008 EOS [5]. For Mixture 3, relative deviations range between (1.16 and 1.43)% and between (1.33 and 2.09)% for Mixture 4. The ARD of the experimental data of Mixture 3 from the GERG-2008 model is –1.36% and 2.98% for Mixture 4. A comparison of the experimental data with results predicted with OilMixProp yields an ARD of –2.62% for Mixture 3 and of 1.46% for Mixture 4. Here, the GERG-2008 EOS represents the data of Mixture 3 better than OilMixProp, but not for Mixture 4, which is also evident from the top panel in Fig. 3.

Fig. 3 (bottom panel) shows the relative deviations for (H_2 + n-C_4H_{10}) mixtures of the measured dew-point pressures and values calculated with the GERG EOS plotted versus the hydrogen vapor mole fraction for values measured in this work and for relevant VLE data retrieved from literature (see Table 4). In general, the relative deviations of experimental dew-point pressures from literature [38–41] in comparison with values predicted with the GERG-2008 EOS scatter widely, with the majority deviating up to 60%. Relative deviations greater than 60% are not presented in Fig. 3 to provide a better visualization. For similar temperatures and hydrogen mole fractions, the data published by Klink *et al.* [38] (T = 327 K, y_{H2} = (0.92–0.94)) are in good agreement

with our new experimental data, but show much higher relative deviations in dew-point pressures for temperatures and hydrogen mole fractions outside this range. Data reported by Aroyan and Katz [40] show some overlap in relative deviation of experimental values compared to values calculated with the GERG-2008 EOS [5] at similar (T, y_{H2})-conditions, but to a large extent exceed the uncertainty of the EOS and data measured in this work, without an identifiable pattern. Overall, the dew points determined in the current work are, for the most part, better than and only partially consistent with those reported in the literature (H_2 + n-C_4H_{10}) mixtures.

5. Conclusions and Outlook

In this work, we present dew-point measurements of four hydrogen-rich binary mixtures containing hydrocarbons measured with a microwave re-entrant cavity system. For this purpose, an existing microwave-based apparatus was modified and upgraded. The main modifications include the integration of a new vector network analyzer (VNA) and a syringe pump to achieve higher pressures, thus expanding the measuring range. The four mixtures were prepared and provided by Air Liquide, including specifications of the combined expanded uncertainties ($k = 2$) in composition. For the (H_2 + C_3H_8) mixtures, Mixtures 1 and 2, the propane mole fractions were stated as (0.09995 ± 0.0005) and (0.1499 ± 0.0015), while for the (H_2 + n-C_4H_{10}) mixtures, Mixtures 3 and 4, the n-butane mole fractions were stated as (0.0513 ± 0.00051) and (0.09888 ± 0.001). Dew points for all binary mixtures were measured along isochoric pathways over the temperature range of (256 to 286) K with pressures up to 6.8 MPa for Mixtures 1 and 2 and pressures up to 2.0 MPa for Mixtures 3 and 4.

The combined expanded uncertainty ($k = 2$) in dew-point temperature and pressure for the propane-containing mixtures, Mixtures 1 and 2, was estimated to be between (0.35 and 2.0) K and (0.005 and 0.030) MPa, respectively. The relative deviations of the new experimental dew points compared to values calculated with the current reference equation of state, the GERG-2008 EOS of Kunz and Wagner [5], agree within −3.0% and 2.9% for Mixtures 1 and 2, which is clearly within the uncertainty of 5% reported by the authors of the EOS. Related data found in the literature [34–37] scatter widely, and the dew points determined in this work are partially consistent with, but to a large extent, better than, those reported in the literature. For the butane-containing mixtures, Mixtures 3 and 4, the combined expanded uncertainty ($k = 2$) in dew-point temperature and pressure was estimated to be between (0.38 to 0.58) K and (0.001 to 0.004) MPa, respectively. The relative deviations of the experimental dew-point pressures from values calculated with the reference EOS GERG-2008 by Kunz and Wagner [5] agree within 5.5% for Mixture 3 and 3.7% for Mixture 4. Although the relative deviations for Mixture 3 are slightly outside the uncertainty of 5% reported by Kunz and Wagner [5], those for Mixture 4 are well within 5%. Compared to VLE data found in the literature for (H_2 + n-C_4H_{10}) mixtures [38–41], which are widely scattering and, to a large extent, exceed the uncertainty of the GERG-2008 EOS [5], the experimental dew points determined in this work are mostly better than those reported in the literature. Furthermore, the new experimental data were compared to values calculated with a new cubic EOS developed by Yang *et al.* [24] (with binary interaction parameters for the considered binary systems set to zero) as implemented in the software package OilMixProp 1.0 [43]. As a result, the predictions with OilMixProp represent the experimental data mostly better than the GERG-2008 EOS.

During the experiments and the associated exposure of pressure sensors to hydrogen, a reversible shift in pressure measurement was observed. While no distinct patterns could be identified in the course of this work, the impact of hydrogen on the pressure measurement and, hence, the uncertainty budget is unequivocal. With these findings, the authors encourage further investigation on this matter as a crucial and inevitable part of improving thermophysical property data of hydrogen and hydrogen-rich mixtures. Despite this need and as a suggestion for data improvement, the new experimental data generated in this work shall be used to improve thermodynamic models, e.g., for the development of binary-specific departure functions. As a second source of data improvement, optimization of the experimental apparatus is proposed. This includes the development of enhanced microwave cavity geometries better suited for dew-point investigation, i.e., an improved electromagnetic field distribution with a localized and clearly distinct microwave signal, reduction of the sample volume to minimize the quantity of sample needed, and softening of hard transitions and sharp edges inside the resonator to avoid potential demixing of the sample. The former may be addressed by employing a cooling post to force a localized phase boundary crossing at the location within the cavity where the microwave signal is strongest.

Declaration of generative AI and AI-assisted technologies in the writing process

During the preparation of this work, the authors used Grammarly in order to optimize the language quality. After using this tool, the authors reviewed and edited the content as needed and take full responsibility for the content of the publication.

CRediT authorship contribution statement

Yvonne Leusmann: Writing – review & editing, Writing – original draft, Visualization, Validation, Software, Methodology, Investigation, Formal analysis, Data curation. **Sebastian Klink:** Software, Investigation. **David Vega-Maza:** Writing – review & editing, Writing – original draft. **Markus Richter:** Writing – review & editing, Visualization, Validation, Supervision, Resources, Project administration, Methodology, Funding acquisition, Conceptualization.

Declaration of competing interest

The authors declare the following financial interests/personal relationships which may be considered as potential competing interests: Markus Richter reports financial support was provided by EURAMET European Metrology Programme for Innovation and Research. If there are other authors, they declare that they have no known competing financial interests or personal relationships that could have appeared to influence the work reported in this paper.

Data availability

Data are submitted with the paper.

Acknowledgment

Within the project 20IND10 Decarb, this work has received funding from the EMPIR programme co-financed by the Participating States and from the European Union's Horizon 2020 research and innovation programme. The authors thank Dr. Monika Thol of Ruhr University Bochum for supporting the present work with additional literature data. Moreover, the authors are grateful to Dr. Xiaoxian Yang of Chemnitz University of Technology for conducting calculations with the OilMixProp 1.0 software package (contact the corresponding author; it is free for academic institutions). The work concerning the impact of hydrogen on accurate pressure measurement devices was carried out within the Master thesis of Fabian Luther.

Appendix A. Supplementary data

The SI provides numerical values for the experimental data in tables and as machine-readable files provided in the property information format (PIF). Supplementary data to this article can be found online at https://doi.org/10.1016/j.fuel.2024.132583.

References

[1] Algayyim SJM, Saleh K, Wandel AP, Fattah IMR, Yusaf T, Alrazen HA. Influence of natural gas and hydrogen properties on internal combustion engine performance, combustion, and emissions: A review. Fuel Apr. 2024;362:130844.

[2] Atilhan M, et al. Thermodynamic characterization of deepwater natural gas mixtures with heavy hydrocarbon content at high pressures. J Chem Thermodyn Mar. 2015;82:134–42.

[3] Hernández-Gómez R, Tuma D, Lozano-Martín D, Chamorro CR. Accurate experimental (p, ρ, T) data of natural gas mixtures for the assessment of reference equations of state when dealing with hydrogen-enriched natural gas. Int J Hydrogen Energy Dec. 2018;43(49):21983–98.

[4] Lozano-Martín D, et al. Thermodynamic (p, ρ, T) characterization of a reference high-calorific natural gas mixture when hydrogen is added up to 20 % (mol/mol). Int J Hydrogen Energy Jun. 2024;70:118–35.

[5] Kunz O, Wagner W. The GERG-2008 wide-range equation of state for natural gases and other mixtures: an expansion of GERG-2004. J Chem Eng Data Nov. 2012;57 (11):3032–91.

[6] Thol M, Richter M, May EF, Lemmon EW, Span R. EOS-LNG: A fundamental equation of state for the calculation of thermodynamic properties of liquefied natural gases. J Phys Chem Ref Data Sep. 2019;48(3):033102.

[7] Beckmüller R, Thol M, Bell IH, Lemmon EW, Span R. New equations of state for binary hydrogen mixtures containing methane, nitrogen, carbon monoxide, and carbon dioxide. J Phys Chem Ref Data Mar. 2021;50(1):013102.

[8] Beckmüller R, Bell IH, Thol M, Lemmon EW, Span R. New fundamental equations of state for binary hydrogen mixtures containing argon, helium, and neon. Cryogenics Jun. 2024;140:103817.

[9] O. Kunz and European Gas Research Group, Eds., The GERG-2004 wide-range equation of state for natural gases and other mixtures, Als Ms. gedr. in Fortschritt-Berichte VDI Reihe 6, Energietechnik, no. 557. Düsseldorf: VDI-Verl; 2007.

[10] Alanazi A, Ali M, Bawazeer S, Yekeen N, Hoteit H. Evaluation of cubic, PC-SAFT, and GERG2008 equations of state for accurate calculations of thermophysical properties of hydrogen-blend mixtures. Energy Rep Nov. 2022;8:13876–99.

[11] Kandil ME. A Vibrating Wire Viscometer and a Microwave Cavity Resonator for the Measurement of Viscosity, Dew Points, Density, and Liquid Volume Fraction at HIgh Temperature. University of Canterbury, New Zealand, 2005.

[12] Tsankova G, Richter M, Madigan A, Stanwix PL, May EF, Span R. Characterisation of a microwave re-entrant cavity resonator for phase-equilibrium measurements and new dew-point data for a (0.25 argon + 0.75 carbon dioxide) mixture. J Chem Thermodyn Oct. 2016;101:395–404.

[13] Tsankova G, Stanwix PL, May EF, Richter M. Densities, Dielectric Permittivities, and Dew Points for (Argon + Carbon Dioxide) Mixtures Determined with a Microwave Re-entrant Cavity Resonator. J Chem Eng Data Sep. 2017;62(9): 2521–32.

[14] Tsankova G, Richter M, Stanwix PL, May EF. Densities and dielectric permittivities for (carbon monoxide + carbon dioxide) mixtures determined with a microwave re-entrant cavity resonator. J Chem Thermodyn Feb. 2019;129:114–20.

[15] Tsankova G, Leusmann Y, Span R, Richter M. Dew Points, Dielectric Permittivities, and Densities for (Hydrogen + Carbon Dioxide) Mixtures Determined with a Microwave Re-Entrant Cavity Resonator. Ind Eng Chem Res Nov. 2019;58(47): 21752–60.

[16] Rogers WJ, Holste JC, Eubanl PT, Hall KR. Microwave apparatus for phase transition studies of corrosive fluids to 1.7 kbar and 588 K. Rev Sci Instrum 1985; 56:1907–12.

[17] Goodwin ARH, Mehl JB, Moldover MR. Reentrant radio-frequency resonator for automated phase-equilibria and dielectric measurements in fluids. Rev Sci Instrum Dec. 1996;67(12):4294–303.

[18] May EF. An advanced microwave apparatus for the measurement of phase behaviour in gas condensate fluids. The University of Western Australia; 2003. PhD Thesis.

[19] May EF, Edwards TJ, Mann AG, Edwards C. Dew point, liquid volume, and dielectric constant measurements in a vapor mixture of methane + propane using a microwave apparatus. Int J Thermophys Nov. 2003;24(6):1509–25.

[20] Kandil ME, Marsh KN, Goodwin ARH. A re-entrant resonator for the measurement of phase boundaries: dew points for {0.4026CH4+0.5974C3H8}. J Chem Thermodyn Jul. 2005;37(7):684–91.

[21] May EF, Pitre L, Mehl JB, Moldover MR, Schmidt JW. Quasi-spherical cavity resonators for metrology based on the relative dielectric permittivity of gases. Rev Sci Instrum Oct. 2004;75(10):3307–17.

[22] Cuccaro R, Gavioso RM, Benedetto G, Madonna Ripa D, Fernicola V, Guianvarc'h C. Microwave determination of water mole fraction in humid gas mixtures. Int J Thermophys 2012;33(8–9):1352–62.

[23] Leusmann Y, Hopkins MG, May EF, Stanwix PL, Richter M. Framework for In situ measurements of vapor-liquid equilibrium using a microwave cavity resonator. Int J Thermophys Jan. 2023;44(1):4.

[24] Yang X, Frotscher O, Richter M. Symbolic-regression aided development of a new cubic equation of state for improved liquid phase density calculation at pressures up to 100 MPa. Int J Thermophys, to be submitted; 2024.

[25] Watson JTR. National Engineering Laboratory. Report prepared for Ruhrgas AG: East Kilbride; 2000.

[26] "LabVIEW." National Instruments Corporation, Austin, TX United States, 2018.

[27] Richter M, Kleinrahm R. Influence of adsorption and desorption on accurate density measurements of gas mixtures. J Chem Thermodyn Jul. 2014;74:58–66.

[28] Lemmon EW, Bell I, Huber ML, McLinden MO. NIST Standard Reference Database 23: Reference Fluid Thermodynamic and Transport Properties-REFPROP. Maryland, USA: Gaithersburg; 2018.

[29] Petersan PJ, Anlage SM. Measurement of resonant frequency and quality factor of microwave resonators: Comparison of methods. J Appl Phys Sep. 1998;84(6): 3392–402.

[30] Bell S. Measurement Good Practice Guide No. 11 (Issue 2). p. 41.

[31] Filliben JJ, McKinney JE. Confidence limits for the abscissa of intersection of two linear regressions. J Res Natl Bur Stan Sect B Math Sci Jul. 1972;76B(3–4):179.

[32] Richter M, Kleinrahm R, Lentner R, Span R. Development of a special single-sinker densimeter for cryogenic liquid mixtures and first results for a liquefied natural gas (LNG). J Chem Thermodyn Feb. 2016;93:205–21.

[33] Bernardini L, Kleinrahm R, Moritz K, McLinden MO, Richter M. The four-sinker densimeter: a new instrument for the combined investigation of accurate densities and sorption phenomena of pure gases and gas mixtures. Int J Thermophys Apr. 2024;45(4):49.

[34] Burriss WL, Hsu NT, Reamer HH, Sage BH. Phase behavior of the hydrogen-propane system. Ind Eng Chem Jan. 1953;45(1):210–3.

[35] Trust DB, Kurata F. Vapor-liquid phase behavior of the hydrogen-propane and hydrogen-carbon monoxide-propane systems. AIChE J Jan. 1971;17(1):86–91.

[36] Williams RB, Katz DL. Vapor-Liquid Equilibria in Binary Systems. Hydrogen with Ethylene, Ethane, Propylene, and Propane. Ind Eng Chem Dec. 1954;46(12): 2512–20.

[37] Bolshakov PE, Linshits LR. Phase equilibria in liquid-gas systems at high pressures. Tr GIAP 1954;3:18–27.

[38] Klink AE, Cheh HY, Amick EH. The vapor-liquid equilibrium of the hydrogen—n-butane system at elevated pressures. AIChE J Nov. 1975;21(6):1142–8.

[39] Nelson EE, Bonnell WS. Solubility of hydrigen in n-butane. Ind Eng Chem 1943;35 (1):204–6.

[40] Aroyan HJ, Katz DL. Low temperature vapor-liquid equilibria in hydrogen-n-butane system. Ind Eng Chem Jan. 1951;43(1):185–9.

[41] Augood DR. The separation of HD and H2 by absorptive fractionation. Trans Inst Chem Eng 1957;35:394–408.

[42] Lozano-Martín D, Moreau A, Chamorro CR. Thermophysical properties of hydrogen mixtures relevant for the development of the hydrogen economy: Review of available experimental data and thermodynamic models. Renew Energy Oct. 2022; 198:1398–429.

[43] Yang X, Richter M. Package for thermophysical properties of oils, common fluids and their mixtures. Ind Eng Chem Res., to be submitted 2024.